Isothermal Titration Calorimetry Studies on the Binding of Amino Acids to Gold Nanoparticles

Hrushikesh Joshi,[†] **Pravin S. Shirude,**[‡] **Vipul Bansal,**[†] **K. N. Ganesh,**[‡] **and Murali Sastry*,**[†]

Nanoscience Group, Materials Chemistry Division, and Organic Chemistry (Synthesis) Division, National Chemical Laboratory, Pune-411 008, India

Received: March 19, 2004; In Final Form: May 19, 2004

Isothermal titration calorimetry (ITC) is a powerful and highly sensitive technique commonly used to study interactions between biomolecules in dilute aqueous solutions, both from thermodynamic and kinetics points of view. In this report, we show that ITC may be used to follow the binding of ligands such as amino acids to the surface of inorganic materials such as gold nanoparticles. More specifically, we have studied the binding of one basic amino acid, lysine, and an acidic amino acid, aspartic acid, with aqueous gold nanoparticles at physiological pH. Strong binding of aspartic acid with the gold nanoparticles under these conditions is indicated by ITC, while weak binding was observed in the case of lysine. The differences in binding are attributed to protonation of amine groups in lysine at physiological pH (pI ∼ 9.4) while they are not protonated for aspartic acid (pI ∼ 2.77). That this is the likely mechanism is indicated by the ITC measurement of binding of lysine with nanogold at pH 11 (when the amine groups are not protonated). The binding of the amino acids with gold nanoparticles has been validated with other techniques such as gel electrophoresis and X-ray photoemission spectroscopy.

Introduction

There is much current interest in metal nanoparticles due to their interesting size-dependent optoelectronic and physico-chemical properties[1] and their potential applications in areas ranging from catalysis[2] to electron microscopy markers[3] to plasmonics.[4] Gold nanoparticles, in particular, enjoy a long history dating back to Roman times and, more recently, to the pioneering work of Faraday on the synthesis of stable aqueous dispersions of gold nanoparticles (gold hydrosols).[5] It is of little surprise, therefore, that there are innumerable recipes in the literature for the synthesis of gold nanoparticles both in water[6] and in nonpolar organic solutions.[7]

In parallel with the development of newer experimental processes for the synthesis of gold nanoparticles of controllable size, monodispersity, and shape, the chemistry related to surface modification of gold nanoparticles has also evinced considerable interest. The ability to modulate the surface chemistry of gold nanoparticles by binding suitable ligands has important applications in many areas such as novel organic reactions,[8] sensors (both inorganic and biological entities), biodiagnostics,[9] drug/DNA delivery,[10] and imaging.[11] While thiol-mediated binding of ligands continues to be the chemistry of choice for gold nanoparticle surface modification,[8,9,12] it is increasingly being recognized that amine groups can bind to gold nanoparticles fairly strongly.[13] Indeed, the strong binding of alklyamines with gold has been used to accomplish the phase transfer of aqueous gold nanoparticles to nonpolar organic solvents.[13d] The demonstration that amine groups bind strongly to gold nanoparticles has enabled surface modification of the nanoparticles with amino acids[14] and proteins[15] with important implications for biomedical applications of such hybrid materials.

Even though a number of ligands with various functionalities have been investigated for complexation with gold nanoparticles, to our knowledge there have been no attempts at directly experimentally estimating the strength and nature of these interactions. Isothermal titration calorimetry (ITC) is an extremely powerful and highly sensitive technique that is capable of measuring the heats of interaction of reacting species in solution and has hitherto been used with great success in the study of interactions between biomolecules in dilute aqueous solutions, both from thermodynamic and kinetics points of view.[16] Inhibitor−substrate interactions,[17] protein−protein interactions,[18] protein−DNA interactions,[19] protein−lipid interactions,[20] protein−ligand interactions,[21] protein−metal ion interactions,[22] and drug−enzyme interactions[23] are some of the biomolecular recognition events that have been studied by ITC. In this report, we demonstrate the first application of ITC in understanding the nature of binding of ligands with gold nanoparticles. More specifically, we have investigated the heats of reaction of one basic (lysine, inset, Figure 1Aa) and one acidic amino acid (aspartic acid, inset, Figure 1Ab) during titration against aqueous gold nanoparticles. Our principle observations are that extremely strong binding of aspartic acid with gold nanoparticles occurs at physiological pH while the binding is much weaker in the case of lysine (the interaction being predominantly electrostatic in this case). ITC studies show that lysine binds strongly to gold at pH 11 (above the pI of lysine), thereby indicating that the amine group in the amino acids is required to be unprotonated for strong binding to occur. The complexation of the different amino acids with the gold nanoparticles has independently been studied by X-ray photoemission spectroscopy (XPS) and gel electrophoresis and compared with the ITC results. These studies indicate that while ITC can be used to probe strong interactions of ligands with gold nanoparticles, the absence of ITC-sensitive signatures cannot be construed to indicate a lack of ligands on the surface.

---

* To whom all correspondence is to be addressed. E-mail: sastry@ems.ncl.res.in.

† Nanoscience Group, Materials Chemistry Division.

‡ Organic Chemistry (Synthesis) Division.
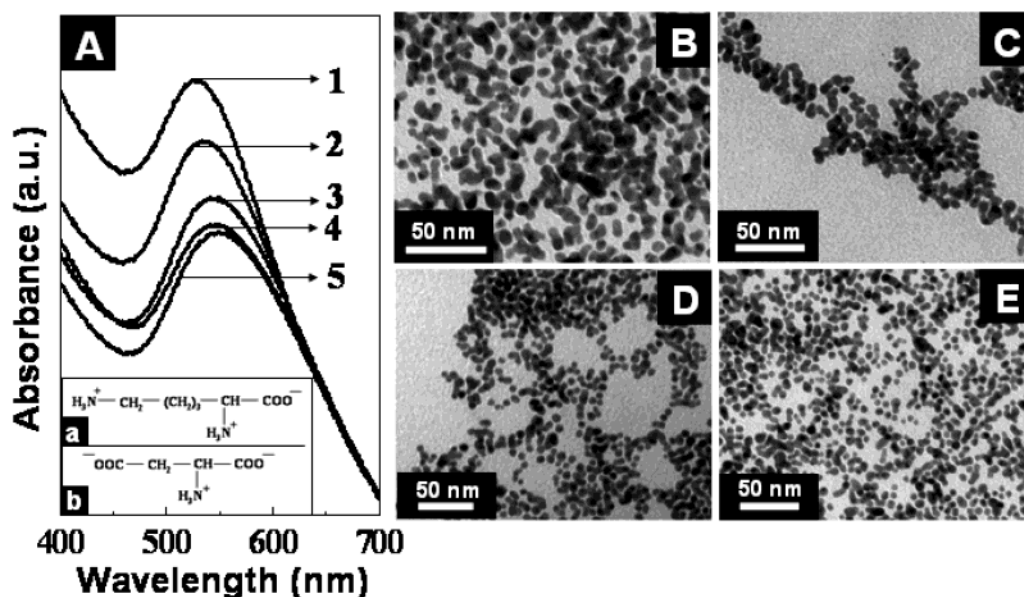
Figure 1. (A) UV–visible spectra recorded from dialyzed borohydride-reduced gold (curve 1), partially capped Au–Asp (curve 2), fully capped Au–Asp (curve 3), Au–Lys pH 7 (curve 4), and Au–Lys pH 11 (curve 5). The inset shows the structural formulas of aspartic acid and lysine. (B–E) Representative TEM images recorded from the as-prepared borohydride-reduced gold nanoparticles; aspartic acid-capped gold nanoparticles; lysine-capped gold nanoparticles at pH 7 and lysine-capped gold nanoparticles at pH 11, respectively.

There is much current interest in interfacing inorganic nanoparticles with biologicals such as amino acids,[14,24] proteins/antibodies,[15,25] and DNA[26] for biodiagnostic and therapeutic applications, and developing methodologies for estimating directly the strength and nature of interactions between amino acids and gold nanoparticles represents an important first step in this direction. Presented below are details of the investigation.

Experimental Section

Reagents and Materials. Chloroauric acid (HAuCl$_4$), sodium borohydride, lysine, aspartic acid, agarose, Tris base, boric acid, and ethylenediamine tetraacetic acid (EDTA) were obtained from Aldrich Chemicals and used as-received. Dialysis membrane (12 kDa cutoff), obtained from Aldrich Chemicals, was used after boiling twice for 5 min followed by thorough washing with deionized water.

Synthesis of Amino Acid-Capped Aqueous Gold Nanoparticles. In a typical experiment, aqueous gold nanoparticles were synthesized by borohydride reduction of chloroauric acid (10^{-4} M of aqueous solution of HAuCl$_4$) in a manner similar to that described earlier.[27] This procedure results in a ruby-red solution containing gold nanoparticles of dimensions 65 ± 7 Å. The colloidal gold solution was dialyzed for 24 h in deionized water using dialysis membrane to remove the excess free borohydride ions and unreduced chloroaurate ions present in the solution, if any. The dialyzed colloidal gold particles were capped by addition of 5 mL of an aqueous solution of 10^{-3} M lysine to 20 mL of the dialyzed gold hydrosol. After addition of lysine and aging the colloidal gold solution for 12 h, this lysine-capped gold (Au–Lys) solution was again subjected to dialysis to remove uncoordinated lysine molecules. In a similar way, Au–Lys at pH 11 (pH adjusted using NaOH) and aspartic acid-capped colloidal gold solutions (Au–Asp) were also prepared. To prepare partially capped Au–Asp colloidal solution, 1.5 mL of 10^{-3} M aspartic acid aqueous solution was added to 20 mL of the dialyzed gold hydrosol and volume was made up to 25 mL with deionized water. The borohydride-reduced gold solution and amino acid-capped gold solutions were

concentrated by rotavapping at 72 mm and 60 °C prior to further analysis in gel electrophoresis experiments.

Instrumental Methods and Characterization. The uncapped and amino acid-capped gold hydrosols were characterized by UV–visible spectroscopy, transmission electron microscopy (TEM), isothermal titration calorimetry (ITC), X-ray photoemission spectroscopy (XPS), and agarose gel electrophoresis. UV–visible spectra of the various colloidal gold solutions were recorded on a Jasco dual-beam UV–Vis–NIR spectrophotometer (model V-570) operated at a resolution of 2 nm. TEM images of drop-coated films of the as-prepared borohydride-reduced gold nanoparticles and Au–Lys (at pH 7 and 11) and Au–Asp (pH 7) nanoparticles on carbon-coated Cu TEM grids were analyzed on a JEOL model 1200EX instrument operated at an accelerating voltage at 120 kV. ITC experiments were performed using a Micro-Cal VP–ITC instrument at 4 °C, wherein 300 μL of a 10^{-3} M aqueous solution of lysine (pH 7), a 10^{-2} M aqueous solution of lysine (pH 11), and 10^{-3} M and 2×10^{-3} M aqueous solutions of aspartic acid (pH 7) were injected in equal steps of 10 μL into 1.47 mL of dialyzed borohydride-reduced gold hydrosol. Gel electrophoresis experiments were conducted in which 1% agarose gel was prepared in TBE buffer at pH 7.2 (Tris, 0.02 M; borate, 0.1 M; EDTA, 0.001 M). The concentrated solutions of dialyzed borohydride-reduced gold, Au–Lys at pH 7 and 11, and partially and fully capped Au–Asp after rotavapping were loaded in the gel wells. The samples were run under the effect of electric field at 60 V in TBE buffer for 1 h, and the gel image was recorded. Samples for XPS were prepared by drop-coating films of Au–Asp (pH 7) and Au–Lys (pH 7 and 11) solutions on Si(111) wafers and analyzing these films in a VG MicroTech ESCA 3000 instrument at a pressure of better than 1×10^{-9} Torr. For the general scan, C 1s, Au 4f, and N 1s core level spectra were recorded with un-monochromatized Mg Kα radiation (photon energy = 1253.6 eV) at a pass energy of 50 eV and electron takeoff angle (angle between electron emission direction and surface plane) of 60°. The overall resolution was ∼1 eV for the XPS measurements. The core level spectra were background corrected using the Shirley algorithm[28]

Binding of Amino Acids to Gold Nanoparticles

*J. Phys. Chem. B, Vol. 108, No. 31, 2004* **11537**

and the chemically distinct species resolved using a nonlinear least-squares fitting procedure. The core level binding energies (BEs) were aligned with respect to the Au $4f_{7/2}$ binding energy of 84 eV.

Results and Discussion

Figure 1A shows the UV−visible spectra recorded from the partially and fully aspartic acid-capped gold hydrosols and lysine-capped gold hydrosol at various pH values. Curve 1 in the figure corresponds to the spectrum of the gold colloidal solution obtained by borohydride reduction of aqueous chloro-auric acid; curves 2 and 3 are the spectra of gold colloidal solutions after partially and fully capping with aspartic acid, while curves 4 and 5 represent the spectra of lysine-capped gold nanoparticles in water at pH 7 and 11, respectively. A strong absorption in curve 1 at ca. 527 nm is observed that corresponds to excitation of surface plasmon vibrations in the gold nano-particles. When the gold nanoparticles are capped with aspartic acid or lysine, a broadening and red shift of the surface plasmon band is observed (curves 2−5), which indicates surface com-plexation of the amino acids and possibly some aggregation of the gold nanoparticles consequent to surface modification. Interestingly, the spectrum recorded from Au−Lys nanoparticles at pH 11 shows greater broadening and red shift when compared with that of Au−Lys nanoparticles at pH 7. The interaction between aqueous gold nanoparticles and the various amino acids thus appears to be quite complex.

The TEM images recorded from the as-prepared borohydride-reduced gold nanoparticles, Au-Asp (pH 7), Au−Lys nanopar-ticles (at pH 7 and 11) are shown in Figures 1B−E, respectively. A comparison of the images shows that while the average morphology of the particles is spherical and that the overall size distribution is uniform in all the cases, the degree of aggregation of the particles is different in each of the experi-ments. The as-prepared borohydride-reduced gold particles are in close contact after water evaporation (Figure 1B), as is to be expected from the fact that they are not stabilized with an amino acid. The Au−Asp and Au−Lys (pH 7) nanoparticles appear to be assembled into open, string-like structures (Figure 1C,D) and would explain the broadening and shift in the surface plasmon band observed in the UV−vis measurements from these samples (Figure 1A). The extent of aggregation is maximum for Au−Lys at pH 11 (Figure 1E), suggesting a high degree of interparticle hydrogen bonding in this case.

The interaction between aspartic acid (pI 2.77) and lysine (pI 9.4) with gold nanoparticles was studied more directly using isothermal titration calorimetry (ITC). Each negative peak shown in the heat signal curves from Au−Asp (Figure 2A,B) and Au−Lys (Figure 3A,B) represents an exothermic process, which denotes the heat released in one injection of the aqueous amino acid into the gold nanoparticle solution as a function of time. While Figures 2A,B and 3A,B correspond to the raw calori-metric data obtained during titration, Figures 2C,D and 3C,D are plots of the integrated heat response obtained from the raw data plotted against the total volume of amino acid solution added to the reaction vessel containing the aqueous gold nanoparticles. Figures 2C,D and 3C,D would thus correspond to binding isotherms of the amino acid on the gold surface. Unlike in studies on the binding of two reacting species in solution (e.g. protein−substrate reaction), where the binding isotherm can be directly plotted against the molar ratio of reactants in solution,[16] the lack of accurate information on the exact surface area of the nanoparticles (i.e., number of moles of surface gold atoms) precludes plotting the binding isotherms
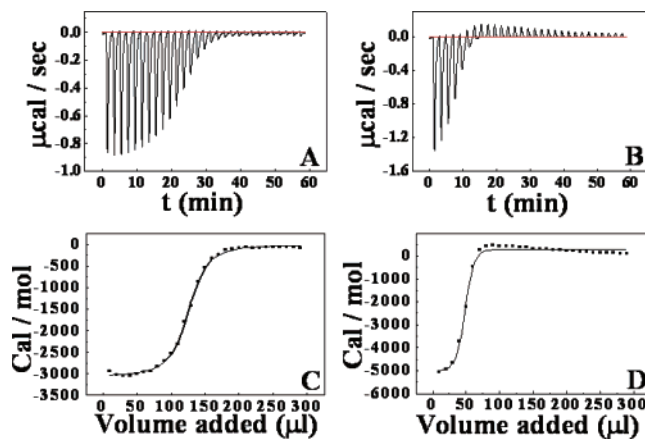
Figure 2. ITC titration data describing the interaction of aspartic acid with gold nanoparticles at physiological pH. Panels A and B show the raw calorimetric data obtained during injection of 10^{-3} and 2×10^{-3} M aqueous aspartic acid solutions into the calorimetric cell containing 1.47 mL of 10^{-4} M gold nanoparticles, respectively. Panels C and D show the integrated data of the curves in panels A and B respectively plotted as a function of total volume of the amino acid solution added to the reaction cell.
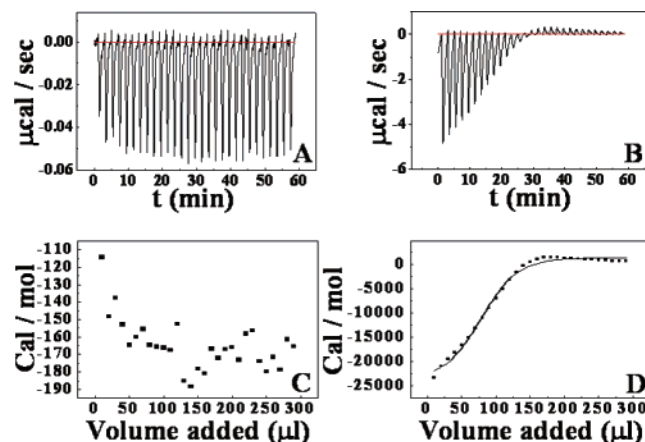
Figure 3. ITC titration data describing the interaction of lysine with colloidal gold nanoparticles at various pH. Panels A and B show the raw calorimetric data obtained during injection of 10^{-3} M and 10^{-2} M lysine solution into the calorimetric cell containing 1.47 mL of 10^{-4} M aqueous gold nanoparticles at pH 7 and 11, respectively. Panels C and D show the integrated data of the curves in panels A and B respectively plotted as a function of total volume of the amino acid solution added to the reaction cell.

against a molar ratio involving the amino acid and gold. Consequently, we have chosen to plot the binding isotherms against the total volume of amino acid added to the reaction cell and will merely use to the data to identify trends in the amino acid binding behavior.

The exothermicity of the calorimetry peaks in Figures 2A,B and 3A,B is believed to be due to the strong interaction between the gold nanoparticles and the amino acids. As the sites available on the surface of the gold nanoparticles become progressively occupied during titration, the exothermicity of the peaks decreases and eventually saturates. The weak endothermic response that is more clearly observed after saturation of the gold nanoparticle surface with the amino acids (Figures 2B and 3B) is believed to arise due to breaking of intermolecular bonds in the amino acids as a consequence of dilution during titration.[29] Parts A and B of Figure 2 show the calorimetric data of reaction of dialyzed borohydride-reduced colloidal gold nanoparticles with 10^{-3} and 2×10^{-3} M aqueous solutions of aspartic acid, respectively (solution pH 7 in both cases). In both cases, strong

binding of aspartic acid with the gold nanoparticles is indicated by the intense exothermic peaks during injection of the amino acid. It is interesting to note that the number of injections required for achieving saturation of the gold nanoparticle surface by aspartic acid in the 10^{-3} M experiment is double that in the 2×10^{-3} M experiment, as would be expected on the basis of the number of available sites for binding and the number of binding molecules. This is more clearly illustrated in the binding isotherms in Figure 2C,D, where the isotherm saturates at 70 μL of aspartic acid in the 2×10^{-3} M experiment while it is ca. 150 μL for the 10^{-3} M experiment. These results clearly show that while accurate quantitative information of the molar ratios of the reacting species is not known in these nanoparticle binding experiments, the trends are quite accurate and, indeed, quantitative.

Figure 3 A shows the calorimetric response of gold nanoparticles during reaction with 10^{-3} M lysine at pH 7. The data obtained show a great deal of scatter with no discernible trend, this being more evident in the corresponding binding isotherm plot (Figure 3C). A comparison of the heats evolved during injection of lysine (Figure 3A) versus that obtained during reaction of gold with aspartic acid (Figure 2A) shows that the binding of lysine with nanogold at pH 7 is extremely weak. It is well-known that amine functional groups bind extremely strongly to gold,[30] our studies indicating that the strength of interaction is comparable to thiol binding with nanogold.[30a] In the comparison between aspartic acid and lysine binding at pH 7 with nanogold, the only difference that could be identified as being responsible for the variation in the strength of binding of the amino acid with gold is the fact that the amine groups would be protonated in lysine at pH 7 (lysine pI 9.4) while they would remain as $-NH_2$ for aspartic acid (aspartic acid pI 2.77). Apparently, the amine groups bind strongly with gold only in the unprotonated state. To test this hypothesis, an ITC measurement of lysine binding with gold nanoparticles at pH 11 was carried out and the data obtained is shown in Figure 3B. At this pH, strong exothermic peaks paralleling aspartic acid binding with gold nanoparticles in intensity are observed for lysine reaction with gold underlining the strong interaction in this case. The binding isotherm for the lysine–gold reaction at pH 11 is shown in Figure 3D clearly showing saturation of the gold surface with lysine after addition of 120 μL of lysine to the reaction cell. At pH 11, the amine groups in lysine would not be protonated and thereby, available for binding to gold nanoparticles. These measurements thus highlight an important criterion for binding of amine-functionalized ligands with gold nanoparticles and establish firmly that the nature of interaction with nanogold is quite strong. At this stage, it is not clear just what kind of bond is formed between the amine groups and the gold nanoparticles, but the nitrogen lone pair electrons are clearly involved.

The ITC measurements indicate strong binding of aspartic acid with gold nanoparticles at pH 7, while the interaction is considerably weaker for lysine under identical conditions. This does not, however, rule out the presence of lysine on the surface of the gold nanoparticles at pH 7 and it was therefore decided to estimate spectroscopically the relative amounts of aspartic acid and lysine present on the gold nanoparticles both at pH 7 and 11. This is conveniently done by X-ray photoemission spectroscopy analysis of films of the amino acid-capped nanoparticles, since XPS is a highly surface sensitive technique. Solution-cast films of Au–Asp at pH 7 and Au–Lys at pH 7 and 11 were formed on Si(111) substrates and analyzed by X-ray photoemission spectroscopy. The general scan spectrum of the
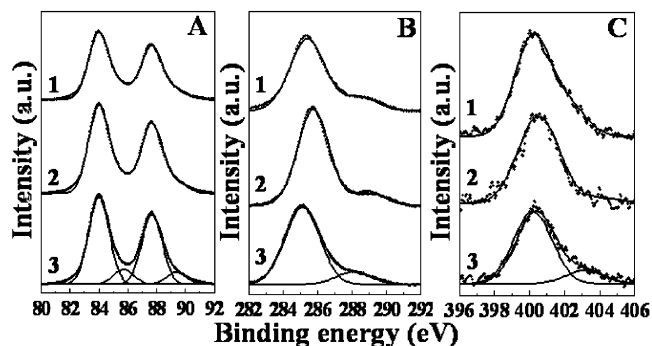
Figure 4. Au 4f (panel A), C 1s (panel B), and N 1s (panel C) core level spectra recorded from amino acid-capped colloidal gold nanoparticles films grown on Si(111) substrates. Curves 1, 2, and 3 in all the panels show spectra recorded from Au−Lys, pH 11 Au−Lys, pH 7; and Au−Asp, pH 7, respectively. The resolved components are shown as solid lines in the figure and are discussed in the text.

films at room temperature showed the presence of C 1s, N 1s, and Au 4f core levels with no evidence of impurities. For XPS analysis, the different core level binding energies (BEs) were calibrated with respect to the Au $4f_{7/2}$ core binding energy of 84 eV. The films were sufficiently thick, and therefore, no signal was measured from the substrate (Si 2p core level). Figure 4A shows the Au 4f core level spectra recorded from Au−Lys at pH 11 (curve 1) and at pH 7 (curve 2) and Au−Asp (curve 3). The spectra have been background corrected using the Shirley algorithm[28] prior to curve resolution. The Au 4f spectrum could be resolved into two spin−orbit pairs (spin−orbit splitting ∼3.68 eV for Au−Asp, 3.708 eV for Au−Lys at pH 7, and 3.670 eV for Au−Lys at pH 11) with the two chemically shifted components having Au $4f_{7/2}$ BEs of 84 and 85.73 eV for Au−Asp, 84 and 85.78 eV for Au−Lys at pH 7, and 84 and 85.70 eV for Au−Lys at pH 11. The low BE component may be assigned to electron emission from Au^0, while the high BE component is attributed to $AuCl_4^-$/$AuCl_2^-$ ions bound to the surface of the gold nanoparticles.[30] In these ions, gold is in the $+3/+1$ oxidation state and appears to a common feature in aqueous borohydride-reduced nanogold formulations.[30] The C 1s core level spectra recorded from Au−Lys at pH 11, Au−Lys at pH 7, and Au−Asp (curves 1, 2, and 3 respectively in Figure 4B) could be decomposed into two peaks located at 285 and 288.4 eV BE and are assigned to hydrocarbons and carboxylate carbons, respectively.[31] The N 1s spectra recorded from Au−Lys at pH 11, Au−Lys at pH 7, and Au−Asp are shown as curves 1, 2, and 3, respectively, in Figure 4C. The N 1s signal in all the cases could be fit to two components, a strong signal centered at 400.3 eV BE and a much weaker peak at ca. 403.2 eV. The low BE peak is quite broad and is assigned to $-NH_2$ and $-NH_3^+$ groups in the two amino acids. At this stage, we are unable to unequivocally assign the 403.2 eV signal. An interesting observation is that the intensities of the N 1s signal in the Au−Lys samples at both pH 11 (curve 1) and pH 7 (curve 2) are quite similar and indeed quite comparable to the N 1s signal recorded from the Au−Asp film (curve 3). Even though the ITC studies indicated weak binding of lysine with gold nanoparticles at pH 7, XPS measurements clearly show the presence of lysine on the gold nanoparticles at concentrations comparable to that observed for lysine binding at pH 11 (and aspartic acid binding at pH 7). A combination of information from ITC and XPS clearly indicates that the interaction of lysine at pH 7 is weak but nevertheless exists to the extent that considerable immobilization of lysine occurs under these conditions. We believe that lysine is bound to the gold nanoparticles electrostatically at pH 7. It is known that boro-

Binding of Amino Acids to Gold Nanoparticles

J. Phys. Chem. B, Vol. 108, No. 31, 2004 **11539**
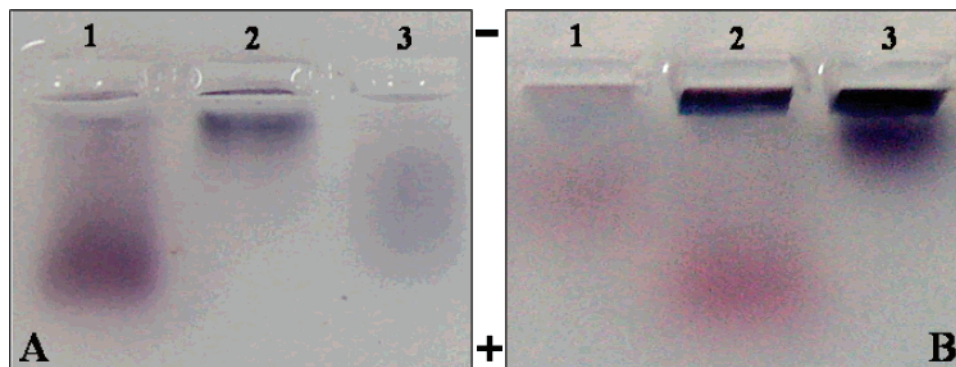
Figure 5. Gel electrophoresis experiment showing the behavior of different charged gold nanoparticles under the effect of an electric field. Panel A shows Au−Lys prepared at pH 11 (lane 1), Au−Lys prepared at pH 7 (lane 2), and borohydride-reduced gold nanoparticles (lane 3) run through the gel. Panel B shows partially capped Au−Asp (lane 1), fully capped Au−Asp (lane 2), and borohydride-reduced gold nanoparticles (lane 3) run through the gel.

hydride-reduced gold nanoparticles are negatively charged at physiological pH due to surface-bound $AuCl_4^-/AuCl_2^-$ ions and that lysine, which would be charged positively at pH 7, could complex electrostatically with the gold surface under these conditions. Weak electrostatic interactions would not be detected by ITC, and hence, as shown in the case of lysine binding at pH 7, caution must be exercised under conditions where interactions are ITC-silent. We would like to stress here that prior to XPS measurements of the Au−Lys and Au−Asp films, the solutions were thoroughly dialyzed to remove uncoordinated amino acid molecules that could interfere with the measurements.

Quantitative estimates of the N/Au ratios were made from the XPS measurements. The values obtained (N/Au, after correction for ionization cross section variation) for the Au−Lys (pH 11), Au−Lys (pH 7), and Au−Asp films are 0.08, 0.15, and 0.10, respectively. Please note that the first two ratios have been divided by two to account for the two amine groups present in lysine as opposed to the one amine group in aspartic acid (inset, Figure 1A). The amount of lysine bound at pH 7 is in fact higher than at pH 11, even though the strength of interaction, determined by ITC, is lower at pH 7. As briefly mentioned earlier, lysine is expected to electrostatically complex with gold ions bound to the surface of gold nanoparticles. In the case of lysine binding at pH 11, the strength of the interaction indicates that it is like a covalent/coordination bond, and therefore, it may be expected to be directional. This would impose steric constraints on lysine binding to the gold surface and therefore limit the coverage of lysine to less than optimum packing values. On the other hand, electrostatic interactions being isotropic would not suffer from such limitations and could thus lead to higher coverages of lysine. This is at best a tentative explanation, and more experiments are required to clarify this issue. The N/Au ratio in the Au−Lys (pH 11) and Au−Asp nanoparticle films are quite similar to each other, indicating roughly the same number of amino acid molecules bound to the surface in each case.

If indeed lysine is bound to the surface of the gold nanoparticles through electrostatic interactions at pH 7, then charge neutralization would occur. In a similar manner, controlling the coverage of aspartic acid on the gold surface would result in an effective variation in surface charge. The ITC measurements of aspartic acid binding to gold nanoparticles indicate that it is indeed possible to control the surface coverage by varying the concentration of aspartic acid added to the reaction medium (Figure 2A,B). These hypotheses may be easily tested by carrying out horizontal gel electrophoretic measurements of the

different amino acid-capped gold nanoparticles at physiological pH. The use of gel electrophoresis in nanoscience is relatively recent and has been applied to separate DNA-capped gold nanoparticles,[32a,b] and protein-capped gold nanoparticles.[32c] During gel electrophoresis, charged nanoparticles may be separated on the basis of their mass and charge on their surface. When lysine-capped gold nanoparticles prepared at pH 7 and 11 were run through the gel along with borohydride-reduced gold (after thorough dialysis, Figure 5A), the Au−Lys nanoparticles prepared at pH 11 (lane 1) showed significantly more mobility toward the anode than both the borohydride-reduced gold nanoparticles (lane 3) and Au−Lys prepared at pH 7 (lane 2). Indeed, there was little movement of the Au−Lys pH 7 sample, indicating almost complete neutralization of the negative surface charge by the electrostatically bound lysine molecules. The larger electrophoretic mobility of Au−Lys pH 11 sample (lane 1) than the borohydride-reduced gold nanoparticles (lane 3) clearly indicates that the negative surface charge in the former case is much higher and arises from the carboxylate ions of lysine, while the smaller negative charge on the borohydride-reduced gold nanoparticles is due to surface bound $AuCl_4^-$ and $AuCl_2^-$ ions.

Figure 5B shows the gel tracks obtained during electrophoresis of partially capped Au−Asp (lane 1), fully capped Au−Asp (lane 2), and as-prepared borohydride-reduced gold nanoparticles (lane 3). The Au−Asp and borohydride-reduced gold nanoparticles move toward the anode, indicating that they are negatively charged. Furthermore, the fully capped Au−Asp nanoparticles have a larger electrophoretic mobility (lane 2) than the partially capped sample (lane 1), as would be expected from the number of carboxylate ions in the amino acid bound to the surface. Thus, differences in surface charge due to variation in coverage of ionized species on nanoparticle surfaces may be monitored quite easily in a standard gel electrophoresis setup.

To conclude, we have shown that isothermal titration calorimetry, a powerful technique normally employed to study biomolecular interactions in solution, may be used to monitor ligand−nanoparticle interactions. Our study of the binding of lysine and aspartic acid as a function of solution pH indicates that the amino acids bind to the gold particles extremely strongly provided the amine groups are unprotonated. Lack of ITC signatures of binding of the ligand to the gold surface should not be construed to indicate a lack of binding of the ligand to the surface—weak electrostatic interactions between lysine and the gold nanoparticles at pH 7 not detected by ITC resulted in significant coverage of the nanoparticle surface by the amino acid. The potential for application of ITC in understanding

phenomena such as ligand binding to nanoparticles and place exchange reactions on nanoparticles[33] is quite exciting, and we hope this work will stimulate interest in this line of research.

References and Notes

(1) (a) Wang, Y.; Herron, N. *J. Phys. Chem.* **1991**, *95*, 525. (b) Colvin, V. L.; Schlamp, M. C.; Alivisatos, A. P. *Nature* **1994**, *370*, 354. (c) Schmid, G., Ed.; *Clusters and Colloids*; VCH: Weinheim, 1994.

(2) (a) Haruta, M.; Kobayashi, T.; Sano, H.; Yamada, N. *Chem. Lett.* **1987**, *2*, 405. (b) Ahmadi, T. S.; Wang, Z. L.; Green, T. C.; Henglein, A.; El-Sayed M. A. *Science* **1996**, *272*, 1924.

(3) Baschong, W.; Wrigley, N. G. *J. Electron. Microsc. Technique* **1990**, *14*, 313.

(4) Maier, S. A.; Brongersma, M. L.; Kik, P. G.; Meltzer S.; Requicha A. A. G.; Atwater, H. A. *Adv. Mater.* **2001**, *19*, 1501.

(5) Faraday, M. *Philos. Trans. R. Soc. London* **1857**, *147*, 145.

(6) (a) Turkevich, J.; Garton, G.; Stevenson, P. C. *J. Colloid Sci.* **1954**, *9*, 26. (b) Handley, D. A. *Colloidal Gold: Principles, Methods and Applications*; Hayat, M. A., Ed.: Academic Press: San Diego, 1989; Vol.1, Chapter 2. (c) Duff, D. G.; Baiker, A.; Edwards, P. P. *Langmuir* **1993**, *9*, 2301. (d) Henglein, A. *Langmuir* **1999**, *15*, 6738. (e) Gachard, E.; Remita, H.; Khatouri, J.; Keita, B.; Nadjo, L.; Belloni, J. *New. J. Chem.* **1998**, 1257. (f) Mizukoshi, Y.; Fujimoto, T.; Nagata, Y.; Oshima, R.; Maeda, Y. *J. Phys. Chem. B.* **2000**, *104*, 6028.

(7) (a) Brust, M.; Walker, M.; Bethell, D.; Schiffrin, D. J.; Whyman, R. *J. Chem. Soc. Chem. Commun.* **1994**, 801 (b) Selvakannan, PR.; Mandal, S.; Pasricha, R.; Adyanthaya, S. D.; Sastry, M. *Chem. Commun.* **2002**, *13*, 1334.

(8) Ingram, R. S.; Hostetler, M. J.; Murray, R. W. *J. Am. Chem. Soc.* **1997**, *119*, 9175.

(9) Storhoff, J. J.; Mirkin, C. A. *Chem. Rev.* **1999**, *99*, 1849.

(10) Niemeyer C. M. *Angew. Chem., Int. Ed.* **2001**, *40*, 4128.

(11) Bielinska, A.; Eichman, J. D.; Lee, I.; Baker, J. R., Jr.; Balogh, L. *J. Nanopart. Res.* **2002**, *4*, 395.

(12) (a) Whetten, R. L.; Khoury, J. T.; Alvarez, M. M.; Murthy, S.; Vezmar, I.; Wang, Z. L.; Stephens, P. W.; Cleveland, C. L.; Luedtke, W. D.; Landman, U. *Adv. Mater.* **1996**, *8*, 428. (b) Johnson, S. R.; Evans, S. D.; Mahon, S. W.; Ulman, A. *Langmuir* **1997**, *13*, 51. (c) Mayya, K. S.; Patil, V.; Sastry, M. *Langmuir* **1997**, *13*, 3944. (d) Liu, J.; Alvarez, J.; Kaifer, A. E. *Adv. Mater.* **2000**, *12*, 1381. (e) Zhang, P.; Kim, P. S.; Sham, P. K. *Appl. Phys. Lett.* **2003**, *82*, 1470.

(13) (a) Leff, D. V.; Brandt, L.; Heath, J. R. *Langmuir* **1996**, *12*, 4723. (b) Brown, L. O.; Hutchison, J. E. *J. Phys. Chem. B.* **2001**, *105*, 8911. (c) Selvakannan, PR.; Mandal, S.; Phadtare, S.; Pasricha, R.; Sastry, M. *Langmuir* **2003**, *19*, 3545. (d) Sastry, M.; Kumar, A.; Mukherjee, P. *Colloids Surf. A*: *Physicochem. Eng. Aspects* **2001**, *181*, 255.

(14) (a) Selvakannan, PR.; Mandal, S.; Phadtare, S.; Gole, A.; Pasricha, R.; Adyanthaya, S. D.; Sastry, M. *J. Colloid Interface Sci.* **2004**, *269*, 97. (b) Mandal, S.; Selvakannan, PR.; Phadtare, S.; Pasricha, R.; Sastry M.; *Proc. Indian. Acad. Sci. (Chem. Sci.)* **2002**, *114*, 513.

(15) (a) Gole, A.; Dash, C.; Soman, C.; Sainkar, S. R.; Rao, M.; Sastry, M. *Bioconjugate Chem.* **2001**, *12*, 684. (b) Phadtare, S.; Kumar, A.; Vinod, V. P.; Dash, C. V.; Rao, M.; Shukla, P. G.; Sivaram, S.; Sastry, M. *Chem. Mater.* **2003**, *15*, 1944.

(16) Jelesarov, I.; Bosshard, H. R. *J. Mol. Recognit.* **1999**, *12*, 3.

(17) Luque, I.; Todd, M. J.; Gomez, J.; Semo, N.; Freire, E. *Biochemistry* **1998**, *37*, 5791.

(18) Thompson, G.; Owen, D.; Chalk, P. A.; Lowe, P. N. *Biochemistry* **1998**, *37*, 7885.

(19) Kunne, A.; Sieber, M.; Meierhans, D.; Allemann, R. K. *Biochemistry* **1998**, *37*, 4217.

(20) Wenk, M. R.; Seelig, J. *Biochemistry* **1998**, *37*, 3909.

(21) Qin, K.; Srivastava, D. K. *Biochemistry* **1998**, *37*, 3499.

(22) Zhang, Y.; Akhilesh, S.; Wilcox, D. E. *Inorg. Chem.* **2000**, *39*, 3057.

(23) Tellez-Sanz, R.; Garcia-Fuentes, L.; Baron, C. *FEBS Lett.* **1998**, *423*, 75.

(24) Zhong, Z.; Patskovskyy, S.; Bouvrette, P.; Luong, J. H. T.; Gedanken, A. *J. Phys. Chem. B* **2004**, *108*, 4046.

(25) (a) Crumbliss, A. L.; Perine, S. C.; Stonehuerner, J.; Tubergen, K. R.; Zhao, J.; O'Daly, J. P. *Biotechnol. Bioeng.* **1992**, *40*, 483. (b) Stonehuerner, J. G.; Zhao, J.; O'Daly, J. P.; Crumbliss, A. L.; Henkens, R. W. *Biosens. Bioelectron.* **1992**, *7*, 421. (c) Zhao, J.; O'Daly, J. P.; Henkens, R. W.; Stonehuerner J. G.; Crumbliss, A. L. *Biosens. Bioelectron.* **1996**, *11*, 493. (d) Mukhopadhyay, K.; Phadtare, S.; Vinod, V. P.; Kumar, A.; Rao, M.; Chaudhari, R. V.; Sastry, M. *Langmuir* **2003**, *19*, 3858. (e) Phadtare, S.; Vinod, V. P.; Mukhopadhyay, K.; Kumar, A.; Rao, M.; Chaudhari, R. V.; Sastry, M. *Biotechnol. Bioeng.* **2004**, *85*, 629.

(26) (a) Elghanian, R.; Storhoff, J. J.; Mucic, R. C.; Letsinger, R. L.; Mirkin, C. A. *Science* **1997**, *277*, 1078. (b) Taton, T. A.; Mucic, R. C.; Mirkin, C. A.; Letsinger, R. L. *J. Am. Chem. Soc.* **2000**, *122*, 6305.

(27) Patil, V.; Malvankar, R. B.; Sastry, M. *Langmuir* **1999**, *15*, 8197.

(28) Shirley, D. A. *Phys. Rev. B.* **1972**, *5*, 4709.

(29) Merino-Garcia, D.; Andersen, S. I. *Langmuir* **2004**, *20*, 1473.

(30) (a) Kumar, A.; Mandal S.; Selvakanna PR.; Pasricha, R.; Mandale, L. E.; Sastry, M. *Langmuir* **2003**, *19*, 6277. (b) Leff, D. V.; Brandt, L.; Heath, J. R. *Langmuir* **1996**, *12*, 4724. (c) Wybourne, M. N.; Hutcchison, J. E.; Clarke, L.; Brown, L. O.; Mooster, J. L. *Microelectron. Eng.* **1999**, *47*, 55.

(31) Sastry, M.; Ganguly, P. *J. Phys. Chem. A.* **1998**, *102*, 697.

(32) (a) Zanchet, D.; Micheel, C. M.; Parak, W. J.; Gerion, D.; Williams, S. C.; Alivisatos, A. P. *J. Phys. Chem. B.* **2002**, *106*, 11758. (b) Sandstrom, P.; Boncheva, M.; Akerman, B. *Langmuir* **2003**, *19*, 7537. (c) Hong, R.; Fischer, N. O.; Verma, A.; Goodman, C. M.; Emrick, T.; Rotello, V. M. *J. Am. Chem. Soc.* **2004**, *126*, 739.

(33) Ingram, R. S.; Hostetler, M. J.; Murray, R. W.; *J. Am. Chem. Soc.* **1997**, *119*, 9175.